A Broadband Planar Magic-T using Microstrip-slotline Transitions

Kongpop U-yen, *Member*, *IEEE*, Edward J. Wollack, *Senior Member*, *IEEE*, John Papapolymerou, *Senior Member*, *IEEE*, and Joy Laskar, *Fellow*, *IEEE*

***Abstract*— The improved version of a broadband planar magic-T using microstrip-slotline transitions is presented. The design implements a small microstrip-slotline tee junction with minimum size slotline terminations to reduce radiation loss. A multi-section impedance transformation network is used to increase the operating bandwidth and minimize the parasitic coupling around the microstrip-slotline tee junction. As a result, the improved magic-T has greater bandwidth and lower phase imbalance at the sum and difference ports than the earlier magic-T design. The experimental results show that the 10 GHz magic-T provides more than 70% of 1-dB operating bandwidth with the average in-band insertion loss of less than 0.6 dB. It also has phase and amplitude imbalance of less than ±1° and ±0.25 dB, respectively.**

***Index Terms*—Microstrip circuits, passive circuits, power combiners, power dividers, slotline transitions.**

I. Introduction

A magic-T is a four-port junction. In an ideal case, it is lossless and has a sum (*H*) port and a difference (*E*) port that allow incident signals from ports 1 and 2 to be combined or subtracted with a well-defined relative phase. See Fig. 1. Structures approximating these ideal properties have been widely used as an element in correlation receivers, frequency discriminators, balanced mixers, four-port circulators, microwave impedance bridges, reflectometers [1] and etc.

A magic-T requires components that are less dependent on transmission phase delay to perform as in-phase and out-of-phase combiners. Structures with high physical symmetry are often used in the magic-T design to produce broadband response with low phase and amplitude imbalance. Symmetry at *H* port is simple to obtain using microstrip line [2] or co-planar waveguide (CPW) [3]. Whereas, symmetry at *E* port is simple to implement using slotline [4] or mode-conversion techniques using slotline structures [4, 5, 6, 7].

On the other hand, magic-Ts with no physical symmetry at *H* or *E* ports require coupled lines [8] or left-handed elements [9] to compensate for phase variations. These magic-Ts can produce broadband response with some tradeoffs in high phase imbalance.

Manuscript received April 15, 2007. Revised August 28, 2007.

K. U-yen and E. J. Wollack are with NASA Goddard Space Flight Center, Greenbelt, MD 20771 USA (phone: 301-286-6233; fax: 301-286-1750; e-mail: kuyen@ pop500.gsfc.nasa.gov).

J. Papapolymerou and J. Laskar are with Georgia Institute of Technology, Atlanta, GA 22305 USA. (E-mail: papapol@ece.gatech.edu).

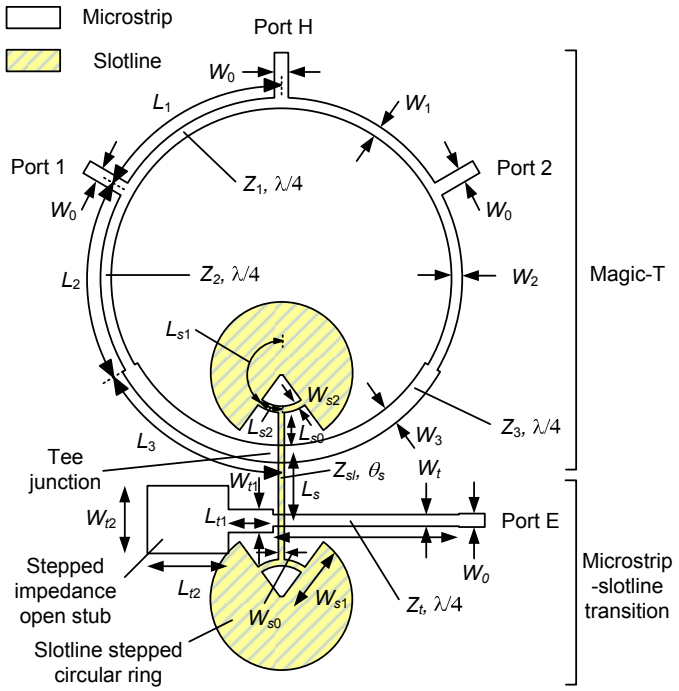

Fig. 1. The improved broadband magic-T using microstrip-to-slotline transitions.

Although the symmetric magic-Ts using the slotline structure have broadband power combining response, their insertion loss, return loss, size and fabrication complexity can limit their usefulness. The total slotline area in these magic-Ts can be large and susceptible to slotline radiation which results in high insertion loss. In addition, magic-Ts using CPW-slotline transition require airbridges to prevent the excitation of undesired modes, which result in extra fabrication steps.

The previously proposed magic-T using microstrip-slotline transitions [7] produces a broad in-phase combining bandwidth using a small slotline area to minimize in-band loss. However, it has a narrowband port 1-2 isolation and port *E*-*E* return loss response. In addition, it is sensitive to microstrip and slotline misalignment. This is due to (1) the limited number of sections of quarter-wavelength (λ/4) impedance transformers used to match all four ports, and (2) the strong parasitic couplings presented at the microstrip-slotline tee junction where four microstrip lines and a slotline are combined. The improved broadband magic-T design,

discussed in this paper, introduces the new microstrip ring structure that minimizes parasitic couplings at the microstrip-slotline tee junction, and simultaneously enhances the return loss at ports 1, 2 and *E* and results in a small phase mismatch. The optimal design of the new structure also increases the overall bandwidth significantly.

II. Circuit Configuration

The improved structure, as shown in Fig. 1, consists of two sections, namely a magic-T and a compact microstrip-slotline transition. The microstrip-slotline transition section has been studied in [7, 10]. This paper focuses on the new approach in designing the magic-T section to simultaneously realize broadband return loss and isolation. The full magic-T transmission line model is also introduced. In addition, the practical upper limit of the magic-T operating bandwidth, designed following this approach, is derived.

The magic-T section in Fig.1 consists of quarter-wavelength (λ/4) microstrip lines connected in a ring configuration. The top section of the ring, above ports 1 and 2, consists of two λ/4 lines with the characteristic impedance of Z_1. It is used as an in-phase combiner with the output port *H* between two Z_1 lines. The bottom section of the ring contains two pairs of λ/4 lines. Each pair contains two microstrip lines with the characteristic impedances of Z_2 and Z_3 connected in series. These lines are used to transform the microstrip to the slotline with the characteristic impedance of Z_{sl}, and produce the microstrip-slotline tee junction at the center of the structure. The Z_{sl} line is terminated with two slotline stepped circular rings (SCRs) at both ends [10] to provide broadband virtual open. Finally, the slotline output is transformed to a microstrip output at port *E* using a microstrip-slotline transition. The magic-T is analyzed in both odd and even modes up to the slotline Z_{sl} section, as shown in Fig. 2(a) and 2(b), respectively.

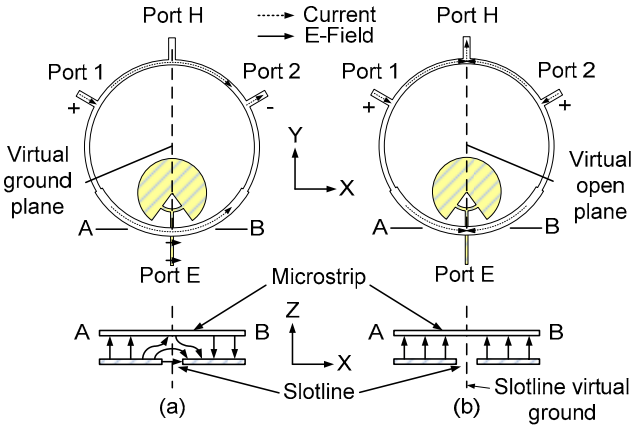

Fig. 2. (a) The odd-mode and (b) the even-mode electric field and current flow in the proposed magic-T and in the microstrip-slotline tee junction at A-B.

In the odd mode, the signals from port 1 and port 2 are out of phase. This creates a microstrip virtual ground plane along the Y-axis of the magic-T and at port *H* as shown in Fig. 2(a). The slotline SCR termination connected to the slotline Z_{sl} allows microstrip-to-slotline mode conversion to occur as indicated by electric field and current directions around the cross-section *A-B*.

In the even mode, the signals from port 1 and port 2 are in-phase, thus creating a microstrip virtual open along the Y-axis of the magic-T as shown in Fig. 2(b). Electric-fields in the slotline at cross-section A-B are canceled, thus creating a slotline virtual ground that prevents the signal flow to or from port *E* by symmetry.

A. Magic-T Circuit Model

The magic-T can be studied using the odd and even modes circuit analysis [7]. By using this analysis and ignoring parasitic reactance due to step in line width, we construct the full circuit model as shown in Fig. 3. This model approximates the magic-T's response around the center frequency f_0.

In the odd mode, the port *H* becomes a virtual ground. Using a λ/4 transformation through Z_1 line, the virtual ground becomes an open at port 1 and port 2, both of which have a characteristic impedance of Z_0. To match the impedance at these ports, λ/4 transmission lines - Z_2 and Z_3 - are used to transform Z_0 to the slot line impedance of $n^2Z_{sl}/2$, where *n* is the microstrip-slotline transformer ratio. In the single mode limit, *n* is dependent on the substrate thickness, the transmission line characteristic impedance and the microstrip-slotline physical alignment [11]. The general equation relating Z_0, Z_2, Z_3, and Z_{sl} can be expressed at f_0 as follows.

$$Z_0 = n^2 \frac{Z_{sl}}{2}\left(\frac{Z_2}{Z_3}\right)^2. \tag{1}$$

It is desirable that $n^2Z_{sl}/2$ equals Z_0 to eliminate the discontinuity of microstrip lines (i.e. Z_2=Z_3). However, in the fabrication process, typically, the value Z_{sl} is limited by the allowable minimum slot width and the substrate thickness. To minimize the radiation loss of the transition, we employ the minimum achievable slotline width (W_{sl}) of 0.1 mm on the 0.25 mm-thick Roger's Duroid 6010 substrate. This slotline width corresponds to a Z_{sl} magnitude of 72.8 Ohm.

In the even mode, port *E* becomes a virtual open and it is half-wavelength transformed to an open at port 1 and port 2. Therefore, there is no constraint on the values Z_2 and Z_3 in this mode at f_0. Moreover, port 1's and port 2's impedances are transformed to $2Z_0$ at port *H* using the Z_1 line. The general solution can be obtained as follows

$$Z_1 = \sqrt{2}Z_0. \tag{2}$$

B. Microstrip and Slotline Transition Terminations

The microstrip-slotline transition in the magic-T requires proper terminations to maintain broad mode-conversion at the microstrip-slotline tee junction and at *E* port. The slotline SCR and the microstrip stepped impedance open stub terminations are used in this section due to its broadband characteristics. In addition, the slotline SCR is more compact and has lower radiation loss than many conventional slotline terminations.

The slotline SCR is modeled using three transmission lines Z_{sl0}, Z_{sl1} and Z_{sl2} with electrical lengths of θ_0, θ_1 and θ_2, respectively [10]. These values correspond to the physical

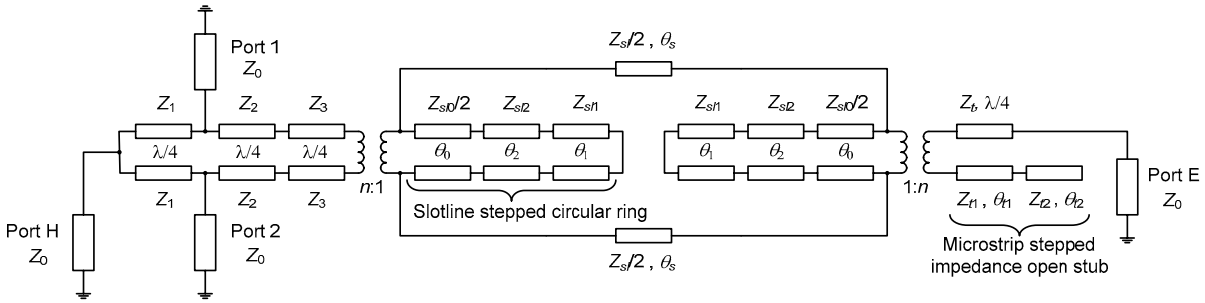

Fig. 3. The full circuit model of the magic-T at the center of the operating frequency.

widths and lengths of W_{s0}, W_{s1} and W_{s2}, and L_{s0}, L_{s1} and L_{s2}, respectively.

The microstrip stepped impedance open stub is modeled using two transmission lines Z_{t1} and Z_{t2} with electrical lengths of θ_{t1} and θ_{t2}, respectively. These values correspond to the physical widths and lengths of W_{t1} and W_{t2}, and L_{t1} and L_{t2}, respectively. The termination models shown in Fig. 3 can be used to accurately determine their frequency responses [10] with the circuit parameter values are provided in Table I.

TABLE I
THE CIRCUIT PARAMETERS AT 10 GHZ USED IN THE MAGIC-T DESIGN ON 0.25 MM-THICK ROGER'S DUROID 6010 SUBSTRATE

Magic-T section		microstrip-slotline transitions
(a) General solution	Z_0=50 Ω, Z_1=70.7 Ω, Z_2=50 Ω, Z_3=42.7 Ω	Z_{t1}=40 Ω, Z_{t2}=20 Ω, Z_t=60.3 Ω, θ_{t1}=24°, θ_{t2}=48°, Z_{sl}=72.8 Ω,
(b) Optimized solution	Z_0=50 Ω, Z_1=57.52 Ω, Z_2=58.9 Ω, Z_3=47.7 Ω	Z_{sl0}=72.8 Ω, Z_{sl2}=72.8 Ω, Z_{sl1}=163.4 Ω, θ_s=31°, n=1, θ_0=14°, θ_1=34.95°, θ_2=6.2°

C. *Magic-T's Optimal Parameter Values*

The general solution based on (1) and (2) is used to construct the magic-T. Using the parameters in Table I(a), the magic-T provides broadband port *E*-*E* return loss and broadband port 1-*E* transmission as shown in Fig. 4(a) and 4(b). However port 1-*H*/2-H transmission and port 1-2 isolation have narrowband response due to all transmission poles are in line at f_0. To increase the return loss and isolation bandwidth of the magic-T, Z_1, Z_2 and Z_3 values can be numerically optimized using a circuit simulation software such that the microstrip line width step discontinuity is more gradual and the port 1-*H*/2-*H* transmission has equal-ripple response. The optimization goal is set to obtain the minimum port *H*-*H* return loss and port 1-2 isolation of 14 dB and 18 dB, respectively, over 70% bandwidth. The frequency responses of the magic-T using the optimized parameters in Table I(b) are shown in Fig. 4(a) and 4(b). The maximum port 1-*H* and 2-*H* transmission bandwidth of the magic-T is limited by strong transmission zeros. These transmission zeros are due to the sections Z_2 and Z_3 as they transform a virtual open at the tee junction to a virtual ground at ports 1 and 2 in the even mode. This is shown in Fig. 4(a) at frequencies f_1 and f_2. Using (3) with Z_2 = 58.9 Ω and Z_3 = 47.7 Ω, we find that f_1 and f_2 are $0.47f_0$ and $1.53f_0$, respectively. The upper port 1-*E* and 2-*E* transmission frequency band is limited by the Z_1

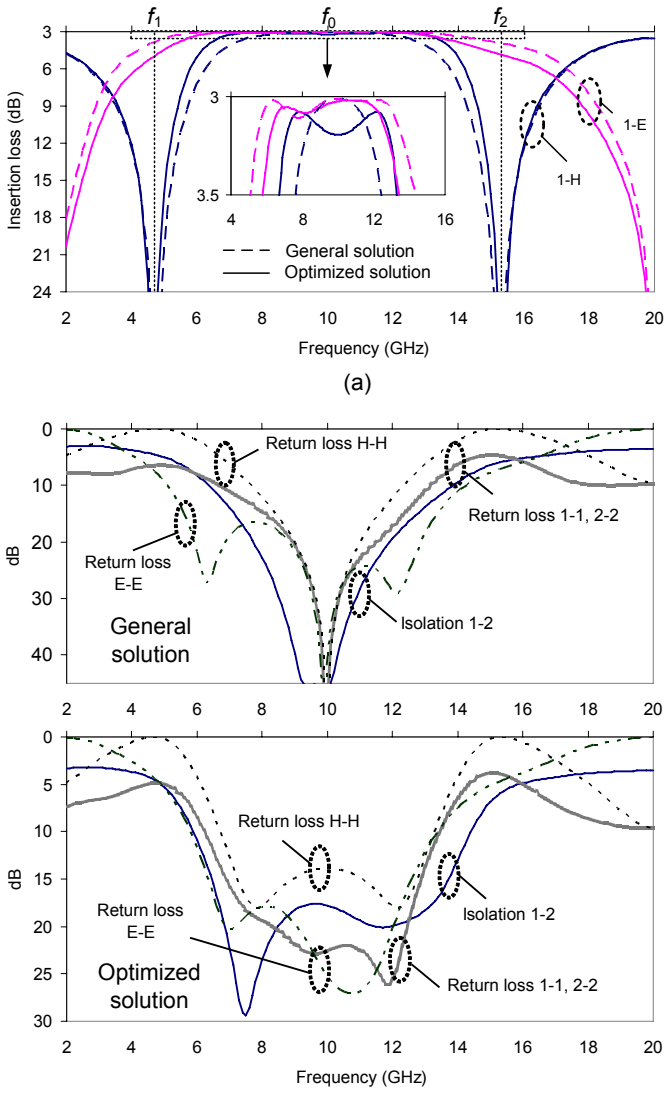

Fig. 4. The magic-T frequency responses of (a) insertion loss and (b) return loss and isolation based on the circuit model shown in Fig. 4 and using the general and optimized solutions provided in Table I. f_0=10 GHz.

$$\frac{f_1}{f_0} = \frac{2}{\pi}\tan^{-1}\left(\sqrt{\frac{Z_3}{Z_2}}\right) = 2 - \frac{f_2}{f_0} \tag{3}$$

section that creates transmission zero at $2f_0$ in the odd mode,since it transforms a virtual ground at port *H* to a virtual open at port 1 or 2. The lower port 1-*E* and 2-*E* transmission

frequency band is limited by the microstrip-slotline transition and tee junction since the slotline SCR termination size becomes so small compared to the slotline wavelength that the slotline SCR effectively becomes a short.

III. Hardware Design And Implementation

A prototype magic-T was fabricated on a 0.25 mm-thick Rogers' Duriod 6010 substrate. The design uses the optimized solution presented in Table I(b) and the corresponding physical parameters of this design are shown in Table II. f_0 is set at 10 GHz. L_s is set to 1.0 mm to minimize slotline radiation loss while obtaining acceptable isolation between the microstrip line at port E and the microstrip-slotline tee junction. Z_{sl} is transformed to Z_0 at port E using a λ/4-long line with an impedance value of Z_t.

TABLE II
THE PHYSICAL PARAMETERS IN MILLIMETER OF THE MAGIC-T ON 0.25 MM-THICK ROGER'S DUROID 6010 SUBSTRATE

Microstrip line sections	Slotline sections
W_0=0.238, W_1=0.175, W_2=0.165, W_t=0.16, L_1=2.92, L_2=2.90, L_3=2.87, L_t=2.79 ,L_{t1}=0.68, W_{t1}=0.37, L_{t2}=1.30, W_{t2}=1.05	L_s=1.0, W_{sl}=0.10, L_{s0}=0.58, W_{s0}=0.10, L_{s1}=0.91, W_{s1}=0.71, L_{s2}=0.23, W_{s2}=0.1

The photographs of the microstrip and slotline sections of the fabricated magic-T are shown in Fig. 5(a) and 5(b), respectively. The magic-T is connectorized and calibrated using the Thru-Reflect-Line method with the reference plane shown in Fig. 5(a) and measured using a Hewlett-Packard 8510C network analyzer. Two magic-T ports are measured at a time while the other ports are terminated with 50 Ohm broadband precision loads. The magic-T provides an average in-band insertion loss of 0.3 dB and 0.6 dB in the in-phase and the out-of-phase power combining sections respectively, as shown in Fig 6(a). The 1-dB corner frequencies of the 1-*H* and 2-*H* transmissions are at 6.6 GHz to 13.6 GHz and the in-band return loss of the magic-T is greater than 10 dB as shown in Fig. 6(b). These measurements are in good agreement with the EM simulations and the circuit response predicted in Fig. 4(a) and 4(b). The 3-dB out-of-phase power combining section has higher insertion loss than the 3-dB in-phase combining section due to additional losses arising from the slotline radiation and microstrip line. The port *E*-*H* isolation is more than 32 dB as shown in Fig. 7. The limit in the port *E*-*H* isolation at low frequency is mainly due to the finite conductivity and the area of ground plane that results in

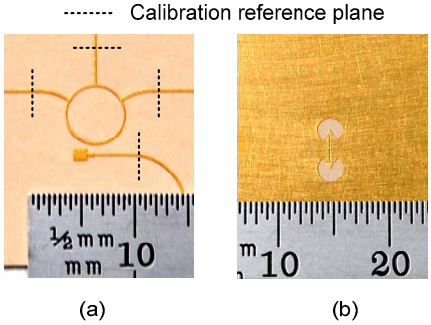

Fig. 5. The photographs show (a) the top and (b) the bottom view of the improved magic-T.

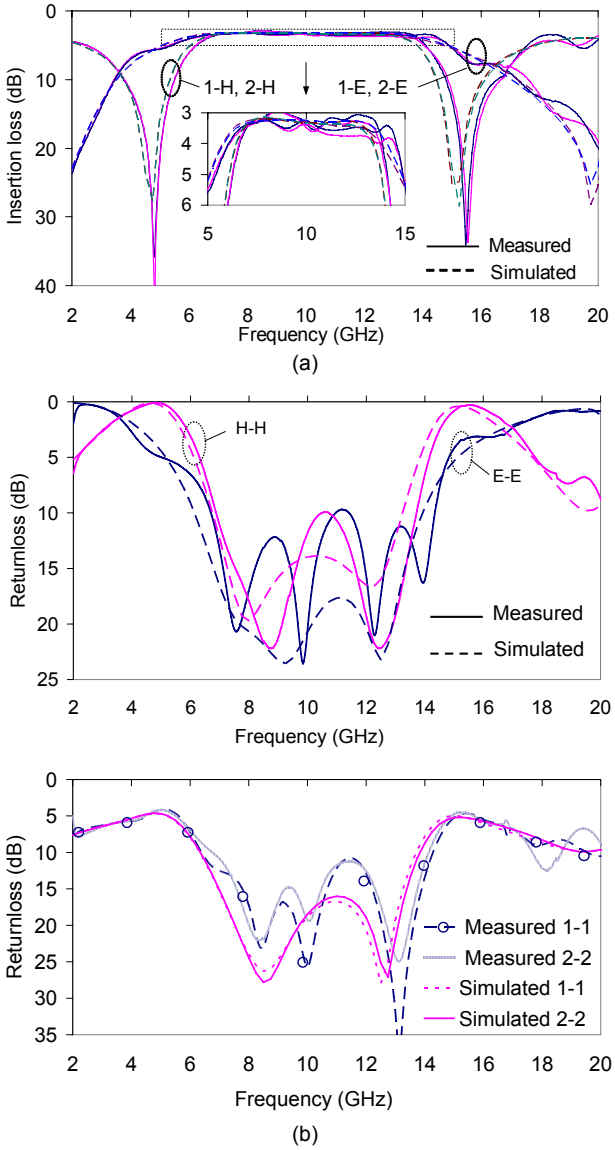

Fig. 6. The measured frequency responses of (a) the insertion loss and (b) the return loss of the optimized magic-T.

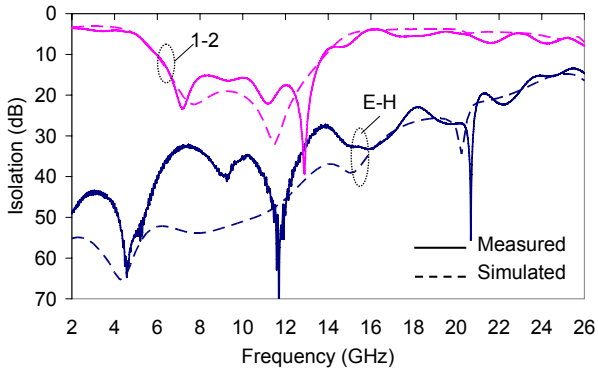

Fig. 7. The measured and simulated isolation at port 1-2 and at port *E*-*H* of the magic-T.

coupling leakage at the microstrip-slotline tee junction. In addition, the amplitude and the phase imbalance of the magic-T is less than ±0.25 dB and ±1 degree as shown in Fig. 8(a)

and 8(b), respectively. Transmission zeros in the magic-T in the port 1-*H* and 2-*H* transmissions result in a sharp increase in phase and amplitude imbalance at f_1 = 4.76 GHz and f_2 = 15.5 GHz. These frequencies are in agreement with those computed using (3). The measurement errors are dominated by the return loss phase and amplitude mismatch at the connectorized broadband load terminations. A secondary error results from the bend line at port *E* which results in perturbation in the phase and impedance mismatch at the reference plane. When compared with the previous design, this magic-T shows significant improvement in bandwidth. The magic-T also has less parasitic around the tee-junction which makes it less sensitive to fabrication misalignment. This results in a much smaller phase imbalance in this design. Their performance comparison is shown in Table III.

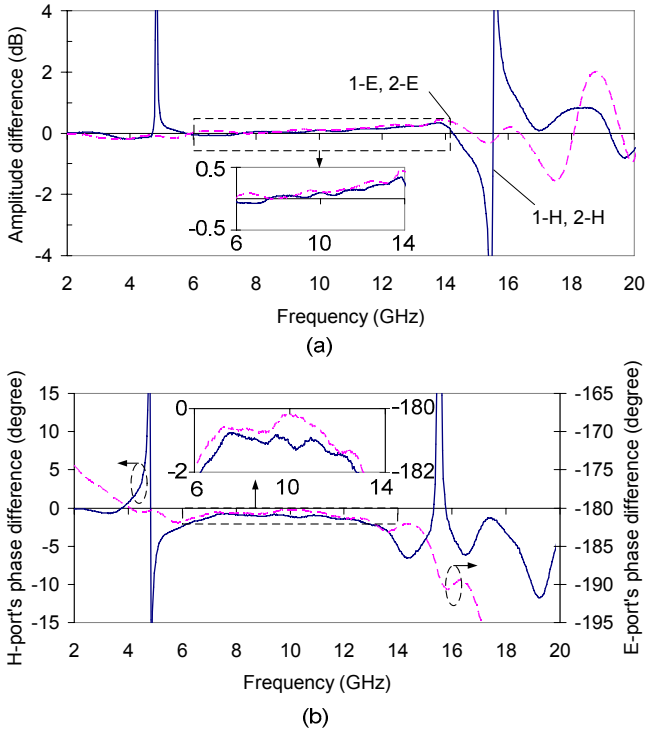

Fig. 8. The measured frequency responses of (a) the amplitude imbalance and (b) the phase imbalance of the optimized magic-T.

TABLE III
SUMMARY OF MEASURED PERFORMANCE OVER 1-dB INSERTION LOSS BANDWIDTH OF THE MAGIC-T COMPARED WITH THE PRIOR MAGIC-T.

	This work	Previous work [7]
Insertion loss (dB)	<0.6	<0.3
1-dB insertion loss bandwidth	75 %	24 %
Phase imbalance	±1 degree	±1.6 degree
Amplitude imbalance (dB)	±0.25	±0.3
Port 1-2 isolation (dB)	>15	>20
Port *E*-*H* isolation (dB)	>32	>31

ACKNOWLEDGMENT

Authors would like to thanks Georgia Electronic Design Center at Georgia Institute of Technology for providing microwave test facilities.

REFERENCES

[1] C. G. Montgomery, R. H. Dicke, and E. M. Purcell, *Principles of microwave circuits*, Chapter 9-12, MIT Rad. Lab Series, McGraw-Hill, vol. 8, 1948.

[2] K. S. Ang, Y. C. Leong, "Converting balun into broad-band impedance-transforming 180° hybrid," *IEEE Trans. Microwave Theory Tech*., vol. 50, pp. 1990-1995, Aug. 2002.

[3] L. Fan, C-H Ho, S. Kanamaluru, and K. Chang, "Wide-band reduced-size uniplanar magic-T, hybrid-ring, and de Ronde's CPW slot couplers," *IEEE Trans. Microwave Theory Tech*., vol. 43, pp. 2749-2758, Dec. 1995.

[4] J. P. Kim and W. S. Park, "Novel configurations of planar multilayer magic-T using microstrip-slotline transitions," *IEEE Trans. Microwave Theory Tech*., vol. 50, pp. 1683-1688, Jul. 2002.

[5] M. Aikawa, H. Ogawa, "A new MIC magic-T using coupled slot lines," *IEEE Trans. Microwave Theory Tech*., vol. MTT-28, pp. 523-528, Dec. 1980.

[6] G. J. Laughlin, "A new impedance-matched wide-band balun and magic tee," IEEE Trans. Microwave Theory Tech., vol. 24, no. 3, pp 135-141, Mar. 1976.

[7] K. U-yen, E. J. Wollack, S. Horst, T. Doiron, J. Papapolymerou, and J. Laskar, "Compact planar magic-T using microstrip-slotline transition," in *2006 IEEE MTT-S Int. Microwave Symp. Dig.*, Hawaii, USA, Jun. 2007.

[8] M. Arain, N. W. Spencer, "Tapered asymmetric magic tee," *IEEE Trans. Microwave Theory Tech*., vol. 23, pp. 1064-1067, Dec. 1975.

[9] H. Okabe, C. Caloz, T. Itoh, "A compact enhanced-bandwidth hybrid ring using an artificial lumped-element left-handed transmission line section," *IEEE Trans. Microwave Theory Tech*., vol. 50, pp. 798-840, Mar. 2004.

[10] K. U-yen, E. J. Wollack, S. Horst, T. Doiron, J. Papapolymerou, and J. Laskar, "Slotline stepped circular rings for low-loss microstrip-to-slotline transitions," *IEEE Microwave Wireless Comp. Lett*., vol. 17, no. 2, pp. 100-102, Mar. 2006.

[11] J. P. Kim and W. S. Park, "Analysis of an inclined microstrip-slotline transition with the use of the spectral-domain immittance approach," *Microwave Opt. Tech. Lett*., vol. 15, no. 4, pp. 256-260, Jul. 1997.

Kongpop U-yen (S'02–M'06) received the B.S. degree in electrical engineering from Chulalongkorn University, Thailand in 1999. He received the M.S. and Ph.D. degrees in electrical engineering from Georgia Institute of Technology in 2002 and 2006, respectively. He was an engineer at L3 communications, California, USA in 2000, where he was responsible for several switching power supply design. In 2001, he joined Texas Instruments where he designed BiCMOS integrated-circuit RF transmitters. At present, he is a senior design engineer at NASA Goddard Space Flight Center in Greenbelt, Maryland, where he has joined since 2004. His research interests are millimeter-wave passive components and RF integrated circuit designs.

Edward J. Wollack (S'85—M'87—SM'98) graduated in 1987 with a B.Sc. in physics and a math minor from the University of Minnesota's Institute of Technology. In 1991 and 1994, respectively, he earned M.Sc. and D.Sc. degrees in physics from Princeton University. In 1994 he began a postdoctoral fellowship at the National Radio Astronomy Observatory, Central Development Laboratory in Charlottesville, Virginia, with a concentration on low-noise millimeter-wavelength detectors and receiver systems for precision continuum radiometry. In 1998, he joined the NASA Goddard Space Flight Center's Laboratory for Astronomy and Solar Physics in Greenbelt, Maryland as an astrophysicist. His research interests include astrophysical and remote sensing, radiometric measurement and calibration techniques, and device noise theory.

John Papapolymerou (S'90–M'99–SM'04) Papapolymerou received the B.S.E.E. degree from the National Technical University of Athens, Athens, Greece, in 1993, the M.S.E.E. and Ph.D. degrees from the University of Michigan, Ann Arbor, in 1994 and 1999, respectively. From 1999-2001 he was a faculty member at the Department of Electrical and Computer Engineering of the University of Arizona, Tucson and during the summers of 2000 and 2003 he was a visiting professor at The University of Limoges, France. From 2001-2005 he was an Assistant Professor at the School of Electrical and Computer Engineering (ECE) of the Georgia Institute of Technology, where he is currently an Associate Professor. His research interests include the implementation of micromachining techniques and MEMS devices in microwave, millimeter-wave and THz circuits and the development of both passive and active planar circuits on semiconductor (Si/SiGe, GaAs) and organic substrates (LCP, LTCC) for System-on-a-Chip/System-on-a-Package RF front ends.

Joy Laskar (S'84–M'85–SM'02–F'05) received the B.S. degree in computer engineering with math/physics minors from Clemson University, Clemson, SC, in 1985, and the M.S. and Ph.D. degrees in electrical engineering from the University of Illinois at Urbana-Champaign, in 1989 and 1991 respectively. Prior to joining the Georgia Institute of Technology, Atlanta, in 1995, he has held faculty positions with the University of Illinois at Urbana-Champaign and the University of Hawaii. At the Georgia Institute of Technology, he holds the Joseph M. Pettit Professorship of Electronics and is currently the Chair for the Electronic Design and Applications Technical Interest Group, the Director of Georgia's Electronic Design Center, and the System Research Leader for the National Science Foundation (NSF) Packaging Research Center. He heads a research group with a focus on integration of high-frequency electronics with opto-electronics and integration of mixed technologies for next-generation wireless and opto-electronic systems. His research has focused on high-frequency IC design and their integration.